Accuracy of distributed optical fiber temperature sensing for use in leak detection of subsea pipelines

S Madabhushi[+], M Z E B Elshafie[*] and S K Haigh[♣]

Abstract

Accurate and rapid detection of leaks is important for subsea oil pipelines to minimize environmental risks and operational/repair costs. Temperature sensing optical fiber cables can provide economic, near real-time sensing of leaks in subsea oil pipeline networks. Employing Optical Time Domain Reflectometry and detecting the Brillouin scattered components from a laser source, temperature gradients can be detected at any location along an optical fiber cable attached to the oil pipeline. The feasibility of such technology has been established in the literature along with a case study on a land-based pipeline. In this paper the accuracy of an optical fiber based temperature sensing system is investigated. A mathematical model which simulates the process of temperature sensing is developed and the results are presented. An experimental investigation is carried out with two different laboratory setups to establish the spatial resolution and accuracy of the optical fiber cable detection system and the experimental results are compared to predictions from the theoretical model. Based on these comparisons it has been established that the optical fiber cable detection system is capable of providing an accurate and rapid assessment of the location of a leak along a subsea pipeline. Furthermore, the sensing system can be used to give an indication of the scale of the oil leak using the temperature gradients detected by the system.

Key words: detection, oil leak, optical fiber, pipeline, subsea

+ Corresponding author, Trinity College, Cambridge, CB2 1TQ (UK)
*University Lecturer, Laing O'Rourke Centre for Construction Engineering and Technology, Department of Engineering, University of Cambridge, Trumpington Street, Cambridge CB2 1PZ (UK)
♣University Senior Lecturer, Department of Engineering, University of Cambridge, Trumpington Street, Cambridge CB2 1PZ (UK)

Introduction

The use of pipelines for the transport of oil, natural gas, water and other fluids has become ubiquitous. Strict standards and regulations are imposed to maintain safe operation of the pipeline networks. Corrosion or other material defects as well as accidental or intentional damage can, however, result in leaks from these pipelines. Walk and Frings (2010) attribute approximately 80% of leaks in 2007 to third-party activities, be they accidental or intentional. The ramifications of pipeline leaks span from environmental damage to severe financial costs. An example of an oil leak from a subsea pipeline is shown in figure 1. This oil leak in the Gulf of Mexico was widely publicized and resulted in both environmental damage and losses to the pipeline operator. The need for accurate and reliable leak detection systems is great, and importantly, rapid detection of leaks can result in large cost savings. Satellite monitoring or local surveys, although feasible, are often both time and labor intensive. Further, these methods often provide only a very localized check on the pipeline, which often extends for several tens of kilometers.

Crude oil is heated before being transported in a pipeline due to the easier transportation of fluids at a lower viscosity. Normally the crude oil is maintained at a temperature between 60^{o}C to 80^{o}C in the pipeline (Mohitpour, 2003). Many pipeline networks are located on the sea bed and are often buried in a shallow trench both to provide protection from anchor and trawl damage and to prevent temperature-induced upheaval buckling of the pipeline (Wang et al. 2012). In this paper only subsea pipelines are considered. When a leak occurs at any section along the pipeline, the escaping oil, which is at a higher temperature than the ambient sea water, creates a plume of fluid with sharp temperature gradients. A system with the ability to accurately detect the spatial location of a leak (using the sharp temperature gradients) as soon as that leak has occurred will help to significantly reduce the associated environmental and cost impacts. Using the principles of Optical Time Domain Reflectometry, by analyzing the Brillouin scattered components from an optical fiber cable attached along the pipeline during construction or retrofitted at a later stage, can provide the required spatial temperature distribution. The distributed (continuous) nature of the fiber optical sensing cables can monitor the temperature profile of the entire pipeline system in almost real-time. If a pipeline leaks at

a specific location and the fluid plume surrounds the optical fiber cable in the vicinity of the leak, the location can be rapidly detected.

Further, it may be possible to infer from the temperature profile measured the scale of the leak, and in this way characterize the urgency of the response required.

Previous research using optical fiber based temperature measurement established the methodology for applying this technique for the detection of oil leaks. Nikles et al (2004) report a case study of successful leak detection in a 55 km long on-shore brine pipeline in Berlin, Germany. A year after construction of the pipeline, excavation work was commissioned close to the pipeline. The construction activity caused a leak that was detected from a large Brillouin frequency shift, triggering an alarm and subsequently stopping the flow through the pipeline.

Selker et al (2006) also detail two case studies of distributed fiber-optic temperature systems. The first was determination of the temperature profile of Lake Geneva and the second was temperature measurements in a decommissioned mine in the Czech Republic. Further, the accuracy of the system was discussed in terms of its agreement with independent measurements obtained by thermocouples in the mine, the system successfully distinguishing 0.01^{o}C changes of temperature with a spatial resolution of 1 m. Walk and Frings (2010) detail potential leak detection system designs, specifically locations of the sensing cable on subsea pipelines. The required temperature differentials for successful leak detection were discussed, concluding that at least 2-5^{o}C changes were required with larger changes giving faster detection times.

The reliability of the leak detection system is inherently dependent on the thermal and spatial resolution of the optical fiber system, including the sensitivity of the cable and reliability of the measurements. The main aim of this paper is to conduct a fundamental study on a typical optical fiber cable to establish its limits of sensitivity and to apply the results to gauge its potential as a leak-detection system for subsea oil pipelines. To this end a series of lab experiments were carried out to measure the spatial and temperature sensitivity. In addition, a mathematical model was developed during the course of this research to simulate the experimental measurements. Comparisons are made

between the experimental results and those from the theoretical model and the result are presented in this paper. The ability of optical fiber cable based temperature measurements to detect temperature changes due to oil leaks affecting small exposed lengths of the cable is investigated.

Brillouin Optical Time Domain Analysis

The glass core in optical fiber cables has an amorphous structure resulting in scattering of light signals sent through them. Whilst in telecommunications this causes attenuation of the useful signal, it is precisely this effect that can be exploited when using optical fiber cables to collect temperature data.

The scattered light can be divided into three main modes. These are known as Rayleigh, Brillouin and Raman scattering. A schematic of these scattering phenomena is shown in Figure 2, where the ordinate of the figure represents intensity of the returning signal. Rayleigh scattering is elastic, and the resulting backscattered light experiences no wavelength change.

As figure 2 illustrates, both modes of inelastic scattering produce backscattered light with frequencies different to the original signal. The Stokes component describes backscattered light which has a lower frequency than the original signal. Similarly the Anti-Stokes component describes backscattered light with higher frequency. Raman scattering can be understood as the absorption or emission of quanta of energy as the material changes its resonant state. As a result, the backscattered light experiences a frequency shift following Planck's Relation. The amplitude of the Stokes component of the Raman scattered light is independent of temperature. However, for the Anti-Stokes component the amplitude of the Raman scattered light is exponentially proportional to the temperature. Therefore, by normalizing the measured intensities of the Anti-Stokes with the Stokes component the temperature at the point of scattering is known. Because Raman-based measurements depend on intensity measurements, they are sensitive to attenuation and not suitable for distances greater than approximately 10 km (Bowley and Sanchez, 1999, Nikles et al, 2004 and Selker et al, 2006).

In general, Brillouin backscattered light arises as a result of density changes in the glass medium of the core. The exact quantum physics explanation is beyond the scope of this paper, however a brief summary will be provided to aid understanding of the apparatus described later. A change of density

causes a phonon wave to travel through the medium. Brillouin scattering is the interaction of an electromagnetic wave with this density wave; photon-phonon scattering. The frequency at which the backscattered signal is most intense is known as the Brillouin frequency, given by equation 1.

$$v_b = \frac{2nv_a}{\lambda} \qquad \ldots(1)$$

where;

$v_b -$ Brillouin Frequency Shift

$n -$ refractive index of fiber

$v_a -$ Acoustic Velocity (of Phonon wave)

$\lambda -$ Wavelength

Frequency shifts arise as a result of a Doppler shift because the signal is backscattered from a moving phonon wave. Importantly, the shift is proportional to the speed of the phonon wave, which in turn is proportional to the density. Therefore, by finding the Brillouin frequency information the local density is known. This can be related to the local temperature and, unlike Raman scattering, to local strain. Therefore equation 1 is modified to give equation 2.

$$v_b(s) = v_{bo} + M\varepsilon(s) \qquad \ldots.(2)$$

where;

$v_b(s) -$ Brillouin Frequency Shift as a function of distance

$v_{bo} -$ Brillouin Shift with zero induced strain

$M -$ Constant of proportionality

$\varepsilon(s) -$ Thermal/ Mechanically induced strain as a function of distance

As Brillouin-based measurements detect shifts in frequency rather than the intensity of the backscattered signals, they allow for measurements over spans greater than 10 km (Chiao et al, 1964, Nikles et al, 2004 and Selker et al, 2006)

Having established that it is possible to determine local properties such as ambient temperature or strain, these can then be combined to create a complete temperature or strain profile along the cable. Optical Time Domain Reflectometry (OTDR) localizes the backscattered signals by measuring the time taken to receive each signal. Given the refractive index, and hence velocity of light in the glass medium, the distance along the medium from which the signal was received can then be calculated using Equation 3.

$$s = \frac{cT}{2n} \qquad \ldots(3)$$

where;

s – Position along fiber

c – Speed of light in a vacuum

T – time period and

n – refractive index of the medium.

Decoupling of the strain and temperature effects is achieved by having the optic fiber cores separated from the protective rubber casing of the cable by a gel layer, isolating them from external strains applied to the cable.

Mathematical Model

The spatial resolution of the analyzer used is quoted as 0.5 m when measuring cables up to 20 m, with the smallest increment given as 0.1 m. These numbers refer to the method by which the analyzer calculates local temperature. The analyzer measures the Brillouin frequency at a maximum of 100,000 points along the cable. However, to improve the accuracy of the measurements, it outputs an average

of these points. Therefore the spatial resolution is given as the distance over which the values are averaged. The increment represents how far along the cable the next average begins. Because the number of measurement points is fixed, the spatial resolution will decrease as the length of the sensing cable is increased. This is an important consideration for applications such as leak detection, where the pipelines are several kilometers long. The spatial resolution decreases to 1 m for a 20 km length, to 2 m at 30 km and 3 m at 50 km lengths (Omnisens, 2009).

In this research, the minimum settings for spatial resolution of 0.5 m and 0.1 m increments were used in order to investigate the limits of the system. Using these settings over longer distances is not a physical limitation, but rather a computational one. Therefore, investigation of the best resolution that the analyzer offers serves as an indication of the potential accuracy of the existing BOTDA system, and can be improved by increasing the number of measurement points in future systems.

Because a moving average is employed, the temperature profile recorded will not necessarily match the actual temperature profile of the cable. Due to the averaging, any peaks of temperature will be spread over a longer length of the cable than is actually heated. Further, if the section of cable heated is less than the spatial resolution, the peak temperature detected will not match the actual peak. The discrepancy will be proportional to the length of the cable actually heated. For a leak detection system, the primary goal would be that any leak induces temperature profiles that are distinguishable from normal ambient temperature values, i.e. the sea water in the cased of subsea pipelines. Further, the ability to estimate the scale of the leak from the temperature profile would also be useful.

To estimate the potential of the system before experiments were conducted, a mathematical model of the analyzer was developed. Given a known applied temperature profile, the model calculates the output temperature profile using an averaging algorithm similar to the one used in the analyzer. One simplification that was made was the analyzers averaging algorithm uses a Lorentzian function to produce a weighted average of the points, whereas the model presented here does not. 100,000 points were used across the length, and the spatial resolution and increment can be set to match the ones in the analyzer. The temperature at any point is given by the formulation shown in equation 4.

$$T(n) = \sum_{j=n-0.5s}^{n+0.5s} \frac{T(j)}{s} \qquad \ldots(4)$$

where;

$$\mathrm{n} - \text{index for point on tempearture profile}$$

$$\mathrm{j} - \text{index in summation}$$

$$\mathrm{s} - \text{spatial resolution}$$

The length of the simulated cable was adjusted to 9 m to accommodate a 3 m spatial resolution. The applied temperature was modelled as a square pulse of magnitude equal to the applied temperature for the exposed length, and ambient temperature elsewhere. Figure 3 shows the expected output from the BOTDA given a fixed length of 0.7 m (from cable length position of 4.175 m to 4.875 m) heated to 70^{o}C and an increment of 0.1 m, whilst varying the spatial resolution from 0.5 m to 3 m. As shown in the figure, the peak temperature is only accurately obtained with the finest spatial resolution, the larger the spatial resolution the larger the discrepancy. Interestingly the drop off in peak temperature detected decays as the spatial resolution is decreased linearly. In addition, the coarser the spatial resolution, the larger the lateral extent of the increased temperature profile. Hence, in terms of detection of a leak, a decreasing spatial resolution would not severely hamper the detection abilities. However, when considering the option of using the measurements to predict the actual thermal conditions such as the peak temperature or lateral extent of the temperature change along the pipe line, low spatial resolutions would not give accurate results.

By default, the increment varies as approximately 1/3 of the spatial resolution. Figure 4 shows the effect of varying the increment in this manner, with the same fixed length of 0.7 m heated to 70^{o}C whilst cycling through the same range of spatial resolutions. It can be observed that with very large increments the shape of the peak detected is heavily distorted. Finally, it should be noted that the combination of a very coarse spatial resolution and large increment may reduce the ability to extrapolate the cable conditions from the profile. This is due to the predicted asymmetry of the

profiles in Figure 4 compared to those in Figure 3. However the ability to just detect an event (oil leak) should remain possible with even using the coarsest settings modelled here.

Experimental Setup

The purpose of this research was to establish the suitability of an optical fiber based system for temperature sensing, specifically its use in leak detection for heated oil pipelines. To this end, sections of optical fiber cables were heated using a body of water. The independent variables were the heated lengths of cable and the temperature that those lengths were exposed to. Cables were given sufficient time to reach thermal equilibrium, so time was not a variable under investigation. However, experiments were carried out to ensure that the exposure time was sufficient for the cable to reach thermal equilibrium. The measurements were recorded using a DiTeSt STA-R analyzer, which uses Brillouin Optical Time Domain Analysis (BOTDA). A 6 m length of EXCEL – SWA loose tube temperature sensing optical fiber cable was connected to the analyzer, via a length of extension cable approximately 800 m long. The specifications of the optical fiber cable are presented in Table 1 (EXCEL – SWA data sheet - 2009).

Two separate experimental setups were used, shown schematically in Figures 5a and 5b. Pictures of the actual setups are shown in Figures 6a and 6b. Figure 6a shows the initial experimental setup when heating lengths of cable from 300 to 1000 mm. Based on the results obtained, the experiment was then extended as seen in Figure 6b, to ascertain the performance of the cable with heated lengths from 10 mm to 200 mm.

Figure 5a shows a water tank with dimensions 525 × 375 × 225 mm. The temperature was set and maintained using a combined heating coil and fan to circulate the fluid. Thermometers were used to measure the temperature and to ensure that the fluid was heated uniformly. A wooden lid was used to hold the coiled cable in the heated water and to prevent heat from the water affecting longer lengths of the outside cable via convection currents in the air. It must be pointed out that specific steps to eliminate conduction were not taken. It was considered that these effects would be insignificant due to

the low thermal conductivity of the optical fiber's rubber casing and the relatively short duration of the experiment.

In Figure 5b the setup for the second experiment is shown. The setup was modified to prevent excessive strain on the optical fiber cables due to small radius coiling when short lengths of the cable were being tested. A short box section of dimensions 200 × 100 × 100 mm was sealed at both ends, and the central plate was moved to vary the heated length of cable. The walls of the box were metal, and some insulation was used around the open length of cable beyond the central plate that was not submerged in water but still enclosed in the box, as shown in figure 6b. This reduced any heating by radiation from the walls of the container.

The DiTeSt analyzer uses BOTDA to identify the Brillouin frequency and hence the temperature and uses OTDR to create a temperature profile along the fiber-optic cable. The analyzer exploits stimulated Brillouin scattering, in which signals are sent from both ends of the cable, the resonant interaction that takes place being measured while varying the frequency. Resonance is a maximum at the Brillouin frequency, so the temperature measurement can be inferred. Although it would be possible to measure the frequency shift of the spontaneously created backscattered light, this represents only a very small proportion of the original signal and accordingly large measurement times (in the order of 30 minutes) are required for accurate readings. By using stimulated Brillouin scattering large signal-to-noise ratios are achieved with relatively short measurement times (5 – 10 minutes), a key advantage for any real-time monitoring system (Chiao et al, 1964).

Experimental Procedure

For the setup shown in figure 5a, the water bath was first heated to the required temperature with a length of optical fiber cable submerged. Three measurements were taken for each heated length between 300 and 1000 mm at 100 mm intervals and at ten temperatures between 25 and 90^{o} C. An average of the three measurements is presented here. All measurements were taken with a spatial resolution of 0.5 m and an increment of 0.1 m. Following a length change, the optical fiber cable was

allowed to reach thermal equilibrium for a period of 4 minutes. For the setup shown in Figure 5b the box was sealed for one length, (200 mm, 100 mm, 50 mm and 10 mm) and the temperature of fluid varied in the same manner as for the previous experiment. The ambient room temperature was maintained constant for all experiments.

As explained earlier, the decision to wait four minutes in order that the cable could reach thermal equilibrium was experimentally validated. Following a length change at a low temperature, the evolving temperature profile was recorded with some results shown in Figure 7. The measurements were taken every minute for 10 minutes. It can be observed that the results do not vary significantly after the first four minutes. For all time increments, the peak applied temperature of 35^{o} C was measured successfully by the system. A time of 4 minutes was thus used for the remainder of the testing reported in this paper. In Figure 7, the apparent variation of the temperature between lengths of 1 m and 2 m is due to mechanical strains in the cable due to the experimental setup. This is, however, outside the region of interest on the cable.

Experimental Results

When considering the experimental results, two important aspects should be taken into account. The first consideration is the ability of any given heated length to produce a noticeable reading when subjected to the various temperatures. In this way, the suitability of the system to pick up an oil leak will be ascertained. Further, depending on the repeatability and sensitivity of the system, it may be possible to deduce from a given measured temperature profile the scale of the leak. It is envisaged that a library of thermal fields induced by various leak sizes could be created. Given the size of a leak, temperature of the leaking fluid and ambient sea temperature, the temperature field created could be modelled. By comparing the trace produced by the system to the library, the scale of the leak could potentially be categorized. This depends highly on the spatial resolution of the detecting system as well as other simplifying assumptions utilized to create the library of leak induced temperature profiles.

Baseline Measurements

The glass cores in the EXCEL – SWA optical fiber cable are suspended in a silica gel. Theoretically this should ensure that no strain is passed from the pipeline to the temperature sensing cable. However by curving the cable at small radii, as shown in Figure 3, it is possible that some strain could be induced in the glass fibers (also see Table 1 for minimum bending radii). Because each length would induce a different curvature, a baseline for each length was recorded. This allowed assessment of the potential for confusion between the thermally and mechanically-induced strains. Some of the results are shown in Figure 8.

From Figure 8 it can be seen that there is a clear peak in strain recorded due to the curvature. This peak is erroneously interpreted as a temperature change. The magnitude of these peaks is, however, very small. As expected, the magnitude of induced strain was inversely proportional to the length of the coiled cable as smaller sections were subjected to greater curvature. As these strain-induced anomalies were small, it was decided to not subtract the additional curvature-induced strains from all the readings, although this should be kept in mind when reviewing the results.

Temperature Sensitivity

The output from the BOTDA for each reading was the three Brillouin frequencies from each repeated measurement, for each 100 mm length along the optical fiber cable. This was converted to give the localized temperature using the equation shown in equation 5.

$$T = 33 + \frac{\left(\sum_{i=1}^{3} \frac{f_i}{3} - 10.86\times10^{9}\right)}{1.05\times10^{6}} \qquad \ldots(5)$$

where;

$f_i -$ Brillouin frequency from each measurment and

T – localized temperature.

The properties of the optical fiber cable used are known and published by the manufacturer. For the cable used in this research, a frequency of 10.86 GHz in response to a 33^{o}C temperature is quoted by EXCEL – SWA Data sheet (2009). This gives a 1.05 MHz change in the Brillouin frequency per 1^{o}C temperature change.

Figure 9 compares the mathematical model and experimental results for a heated length of 900 mm. Similar results were observed for heated lengths of 600, 700 and 800 mm. As one would expect, when the heated length exceeds the spatial resolution of 500 mm, the peak temperature is accurately detected, as seen in Figure 9. The temperature profiles recorded are easily distinguishable and very consistent. An anomaly in the results is the asymmetry of the peaks recorded. As illustrated by the theoretical results, such asymmetry is not expected. Physically this could occur if one side of the optical fiber cable did not reach thermal equilibrium before the measurements were made. However, this is very unlikely in the experimental setup used in this research. Previous research that used this cable also reports this type of asymmetry (Mohammed, 2008) and attributed this to the properties of the specific optical fiber cable. However this aspect needs further research using different types of optical fiber cables.

Although heated lengths of 300, 400 and 500 mm were also tested in the experimental setup shown in Figure 5a, the peak temperature recorded in these cases was smaller than the applied maximum temperature. In order to investigate the ability of the optic fiber cable to detect leaks smaller than the spatial resolution, the slightly modified setup shown in Figure 5b was used. Using this setup, smaller heated lengths of 10, 20, 50, 100 and 200 mm were tested. Figure 10 illustrates that for a heated length of 50 mm, (i.e. the case of a heated length less than the spatial resolution), the peak temperature detected by the optical fiber cable is much smaller than the actual temperature. Whilst the applied temperatures range from 25^{o}C to 90^{o}C, the recorded temperatures range only from 20^{o}C to 30^{o}C, (ignoring the initial apparent temperatures due to the mechanical strains as explained earlier). The recorded profiles are still, however, distinguishable from the baseline readings. This remains the

case for most readings even with a heated length of only 10 mm. The recorded peak for a 30^{o}C heater temperature is of similar magnitude to noise in the readings. A 10^{o}C temperature change over a 50 mm length would thus be a minimum value for successful detection of a small leak. The results of this experiment validate the use of a BOTDA based system to at the very least to detect the presence of a leak at any given location along the pipeline. Although oil pipelines traditionally have an operating range of 60^{o}C to 80^{o}C, a much larger range was investigated in these experiments to validate the full range of possible applications for pipelines carrying other fluids.

Spatial Sensitivity

The ability of the sensing system to accurately distinguish between the different heated lengths of cable underpins the entire premise of determining the severity of a leak detected. This involves both detecting the change in temperature and the lateral extent of the leak. Figure 11 shows the results of the theoretical model and experimental results, given the surroundings were heated to 80^{o}C whilst varying the lengths from 300 to 1000 mm. Similar results were observed for other temperatures tested. As before, the peak temperature was only detected accurately when the heated length exceeded the spatial resolution.

The lateral extent of the leak can be related to the width of the measured temperature profile in Figure 11, (i.e. the wider the temperature profile the larger the lateral extent of the leak). In order to reconstruct the actual lateral extent of the leak from the measured temperature profile, deconvolution is required due to the averaging employed by the BOTDA, (Mohamad, 2008). The clear separation between the measured profiles in Figure 11 gives confidence that a BOTDA based system would be able to accurately detect leak size and location provided that at least a 100 mm of optical fiber cable was exposed to the oil leak. In terms of categorizing the scale of a leak, this is more than sufficient in terms of spatial resolution.

Conclusions

The aim of this paper was to explore the use of a network of distributed fiber optical temperature sensing cables for use in detection of leaks in heated oil pipelines. While previous research in this area

established the theoretical feasibility of using fiber-optic temperature sensing and demonstrated its use in a case study, this research focuses on experimental measurements of the response of the fiber optic cables by heating different lengths of cable to various temperatures. A mathematical model of the Brillouin Optical Time Domain Analyzer used in the experimental research was created to explore the effects of the spatial resolution and increment on any measurements made. This model was used to establish that coarse settings result in the measurement of diminished peaks, although these remain theoretically large enough to detect. The results from the model were then compared with the results from the experimental work. Barring an asymmetry of the peaks detected in the experimental results, possibly due to physical properties of the fiber optical cable used, it was observed that the experimental results obtained were very similar to those obtained from the theoretical model. This theoretical model could thus be used to predict the response of the measurement system under a variety of leak scenarios or to interpret results from a leak detected by the system. In terms of leak detection, even very small exposed lengths (10 mm) exposed to relatively low temperature differentials (10°C) caused peaks easily distinguishable from the baseline measurements. Further, the resolution (resolvability) of the traces given different temperatures and exposed lengths was very good, indicating a system of classifying leak severity using distributed optical fiber temperature sensing cables would be possible.

Acknowledgements

The first author would like to acknowledge the support received under the UROP program from the Centre for Smart infrastructure and construction (CSIC) at the Department of Engineering, University of Cambridge. He would also like to thank the helpful suggestions he received from Mr Chang Ye Gue.

REFERENCES

Bowley, R and Sánchez, M., (1999), Introductory Statistical Mechanics (2nd edition), Oxford: Clarendon Press.

Chiao, R.Y., Townes, C.H. and Stoicheff, B.P., (1964), Stimulated Brillouin scattering and coherent generation of intense hypersonic waves, Physical Review Letters, 12, 592.

EXCEL SWA Fiber-optic cable Data Sheet, (2009), Mayflex, Birmingham, UK. (http://www.mayflex.com/_assets/files/Exc_LT_fiber_SWA_SM_OS1_OS2.pdf)

Goldenberg, S. (2010). BP switches on live video from oil leak. [Online] the Guardian.

Mohamad, H., (2008), Distributed Optical Fiber Strain Sensing of Geotechnical Structures, PhD Thesis, University of Cambridge, UK.

Mohitpour, M., (2003). Pipeline Design and Construction: A Practical Approach. ASME Press. ISBN 978-0791802021.

Nikles, M., Vogel, B., Briffod, F., Grosswig, S., Sauser, F., Luebbecke, S., Bals, A., Pfeiffer, T., (2004), Leakage detection using fiber optics distributed temperature monitoring, Smart Structures and Materials 2004: Smart Sensor Technology and Measurement Systems, 18.

Omnisens, (2009), User Manual DITEST^{TM} Data Viewer, Omnisens SA, Morges, Switzerland.

Selker, J S., Thévanaz, L., Huwald, H., Mallet, A., Luxemburg, W., Giesen, N., Stejskal, M., Zeman, J., Westhoff, M., Parlange, M B., (2006), Distributed fiber-optic temperature sensing for hydrologic systems, Water Resour. Res., 42, W12202, doi:10.1029/2006WR005326.

Walk, T. and Frings, J., (2010), Fiber optic sensing can help reduce third-party threats, Oil & Gas Journal, 108.

Wang, J., Haigh, S.K., Forrest, G. and Thusyanthan, I.T. (2012), Mobilization distance for upheaval bucklingo shallowly buried pipelines, Journal of Pipeline Systems Engineering and Practice, 3(4), 106-114.

Table-1
Click here to download Table: Table1.docx

Table 1 Specifications of the fibre-optic cable

Property	**Value**
Nominal and Maximum Outside Diameter	9.6 / 9.9 mm
Loose Tube Diameter	2.8 ± 0.1 mm
Energy of flame	1509 kJ/m
Weight	237 kg/km
Standard delivery length	2100 ± 100 m 4100 ± 100 m
Temperature range Transport / Storage Installation Operation	 -30 to +70°C -5 to +50°C -30 to +70°C
Pulling tension Long term Short term	 ≤ 700 N ≤ 1500 N
Bending radii for fibres and tubes Installation/operation	 >25 mm
Optical Performance	
Modal-Field Diameter	9.2 ± 0.4 µm 125 ± 0.7 µm
Average Attenuation	0.32 dB/km
Maximum Attenuation	0.40 dB/km
Dispersion	≤ 3.5 $ps.nm^{-1}$ km^{-1}
PMD	≤ 0.2 ps km^{-1}
Cable cut-off wavelength	≤ 1260 nm

Figure-1
Click here to download high resolution image

Figure-2
Click here to download high resolution image

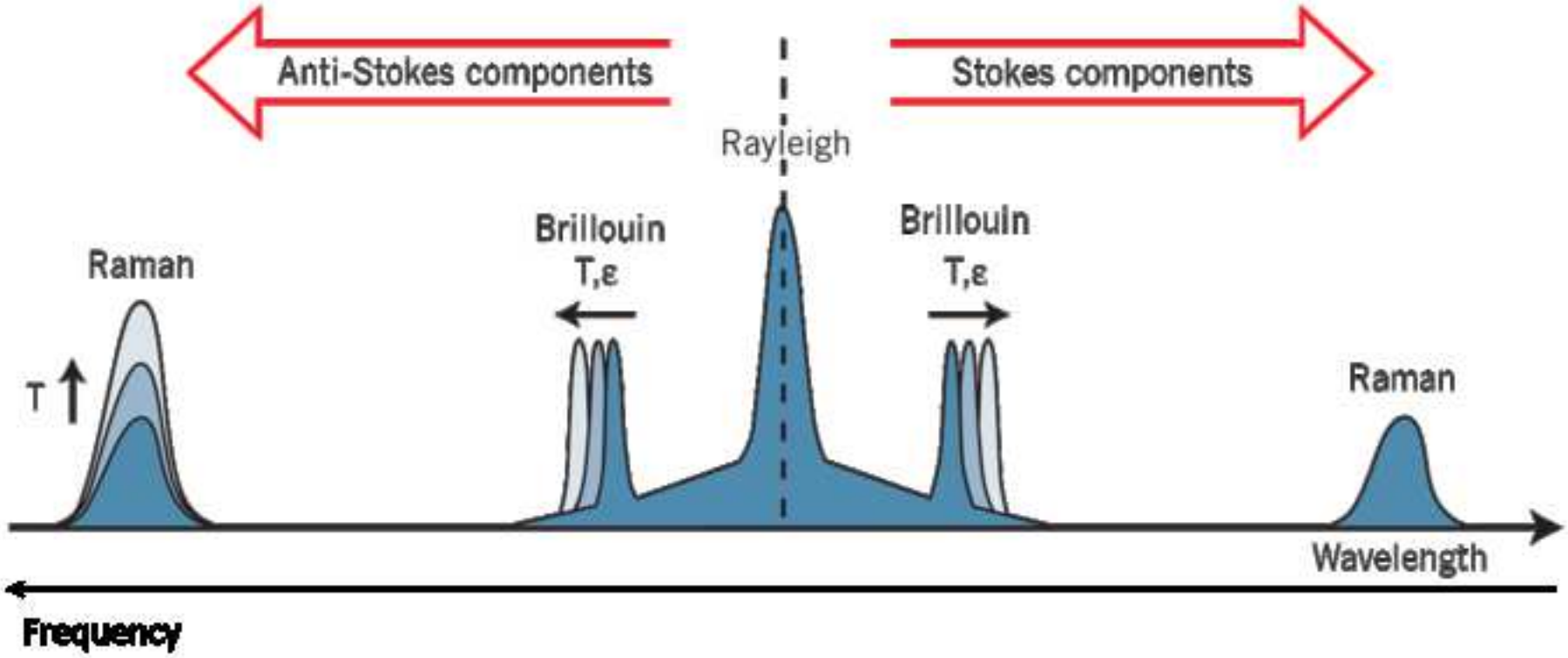

Figure-3
Click here to download high resolution image

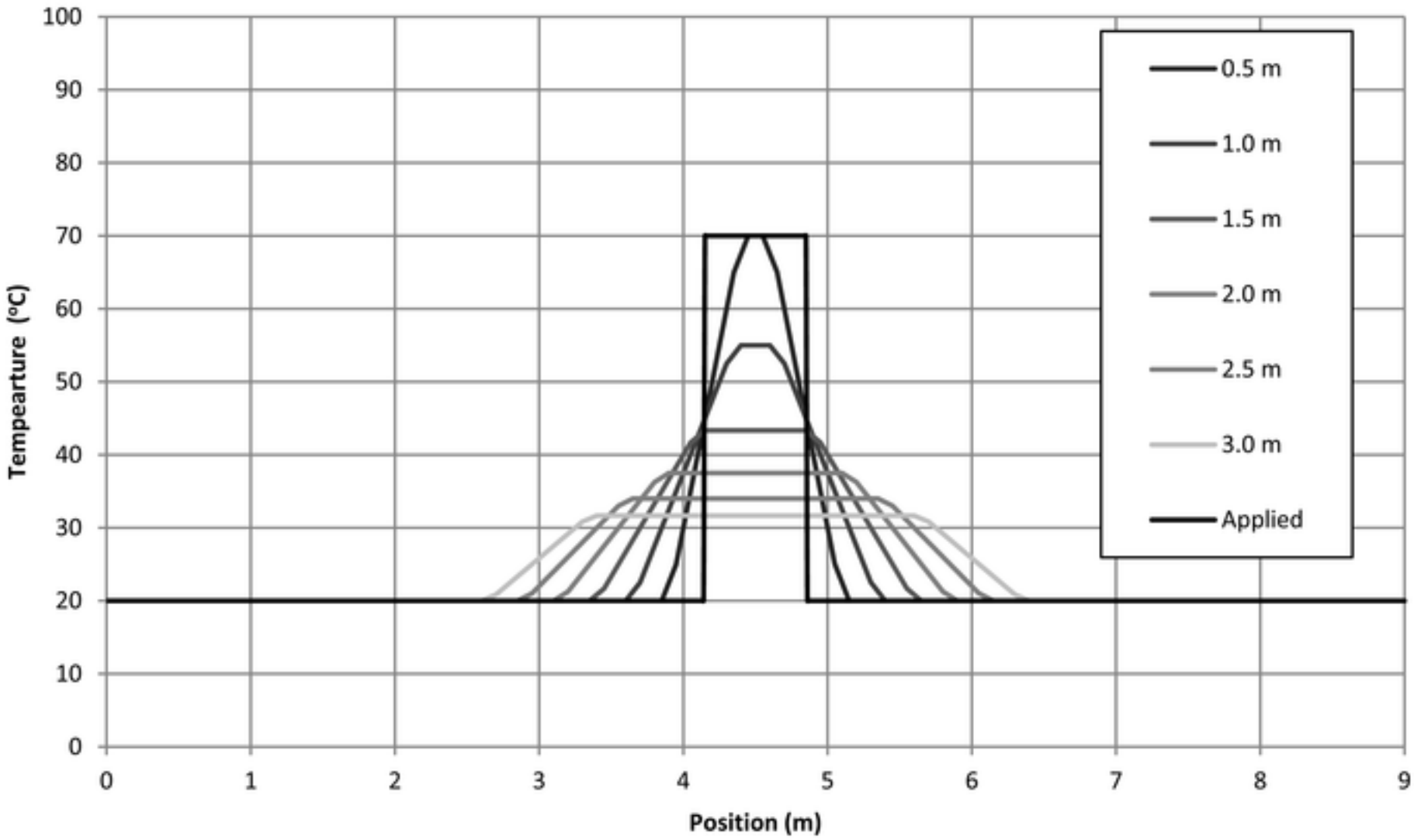

Figure-4
Click here to download high resolution image

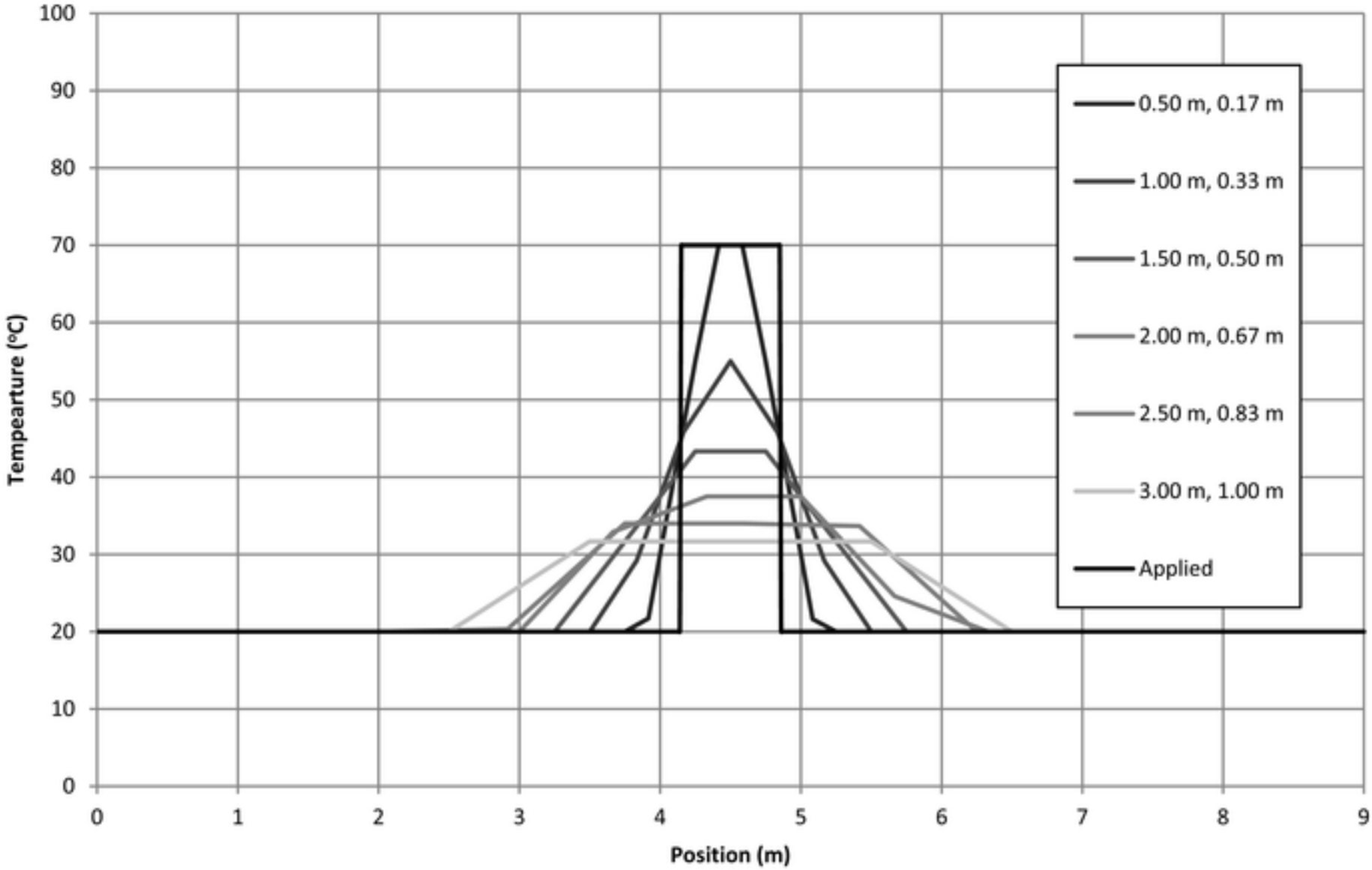

Figure-5
Click here to download high resolution image

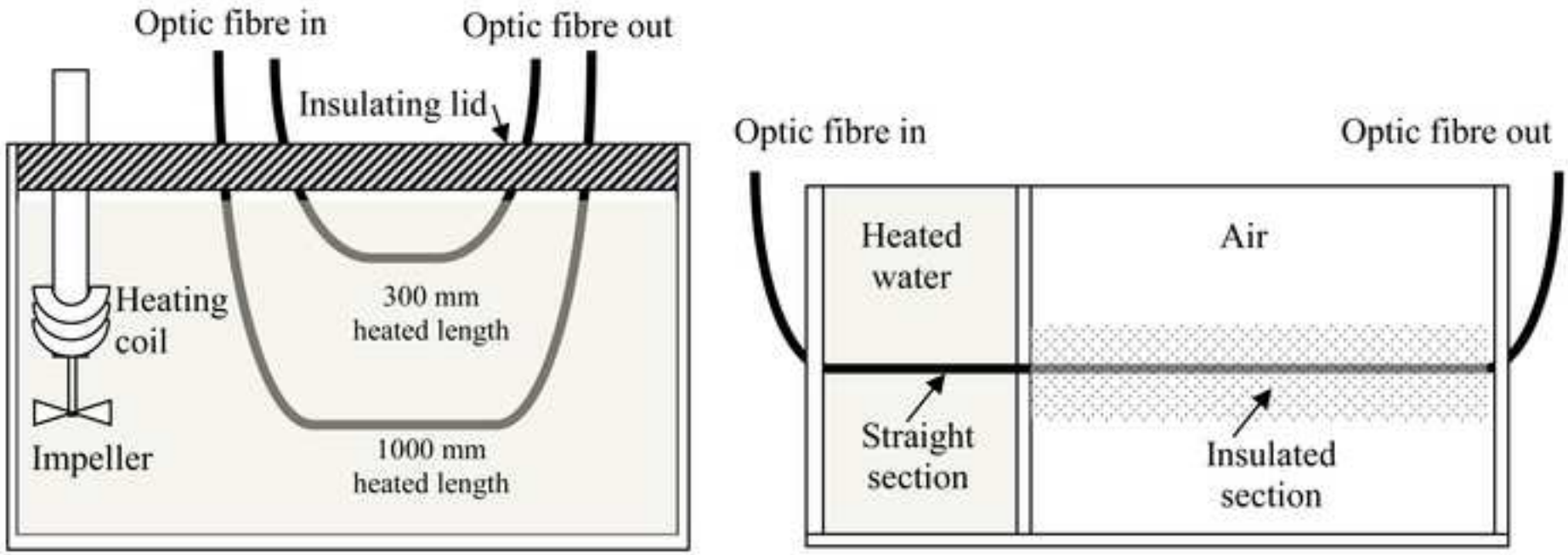

Figure-6
Click here to download high resolution image

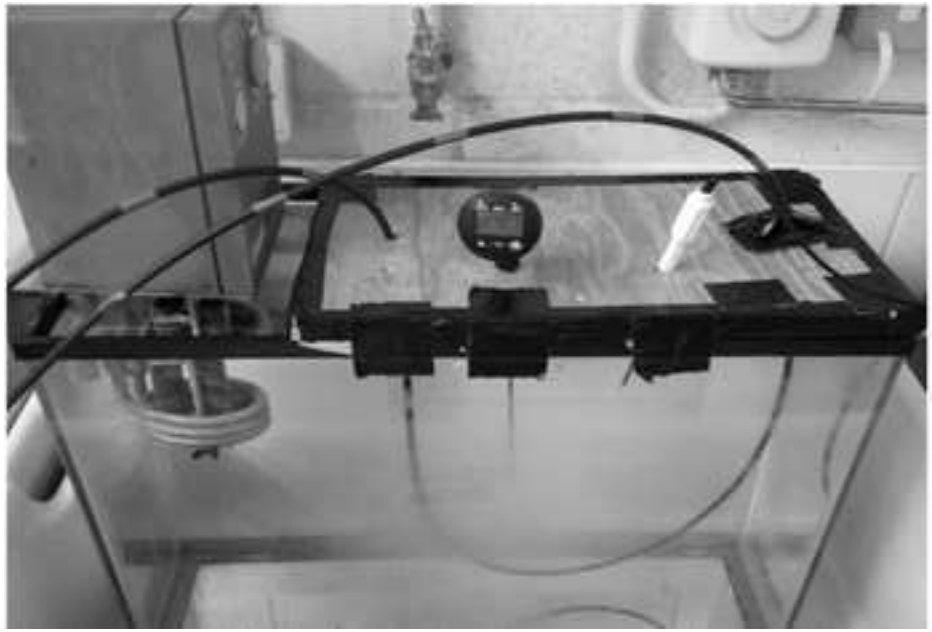

Figure-7
Click here to download high resolution image

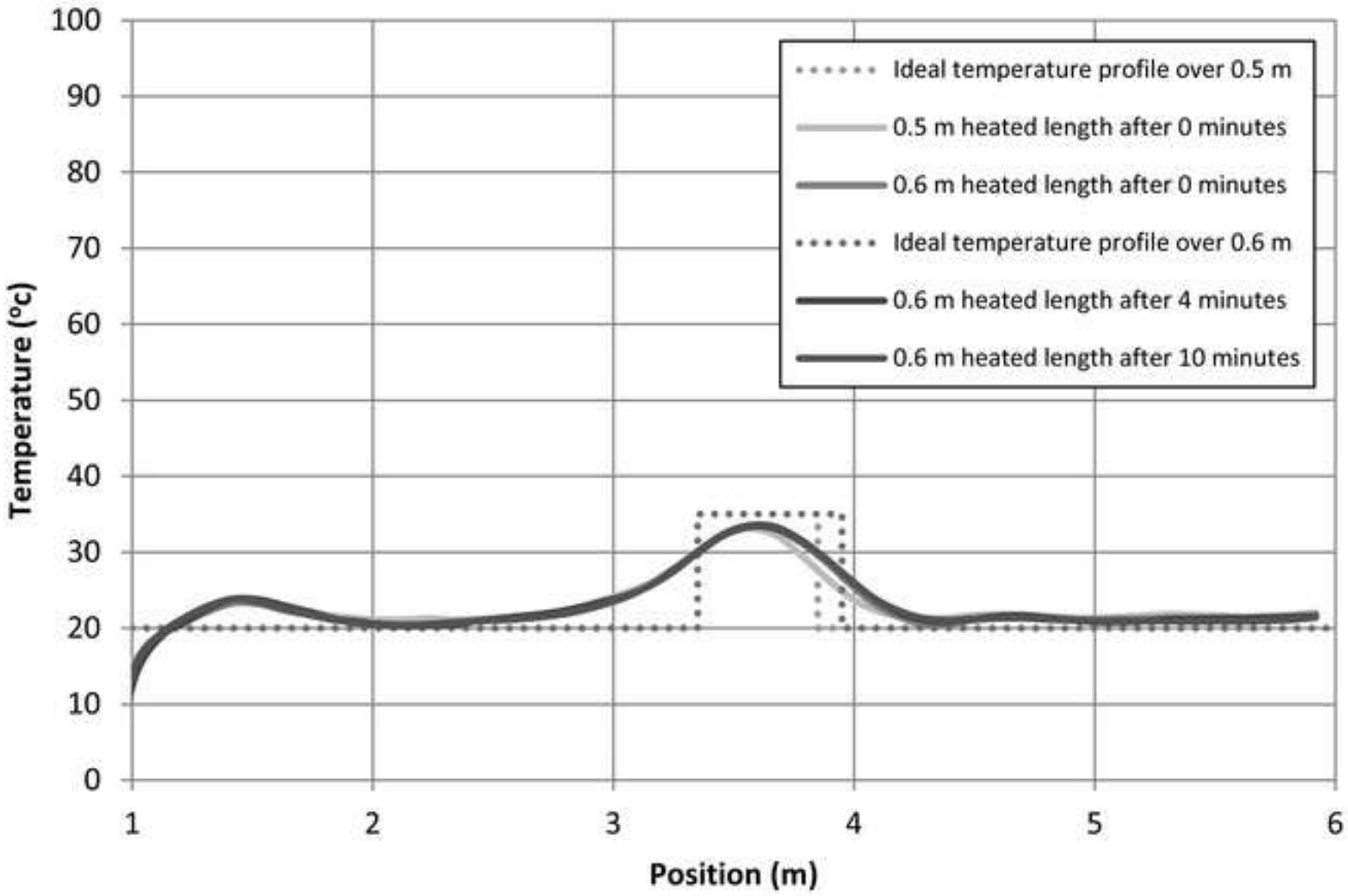

Figure-8
Click here to download high resolution image

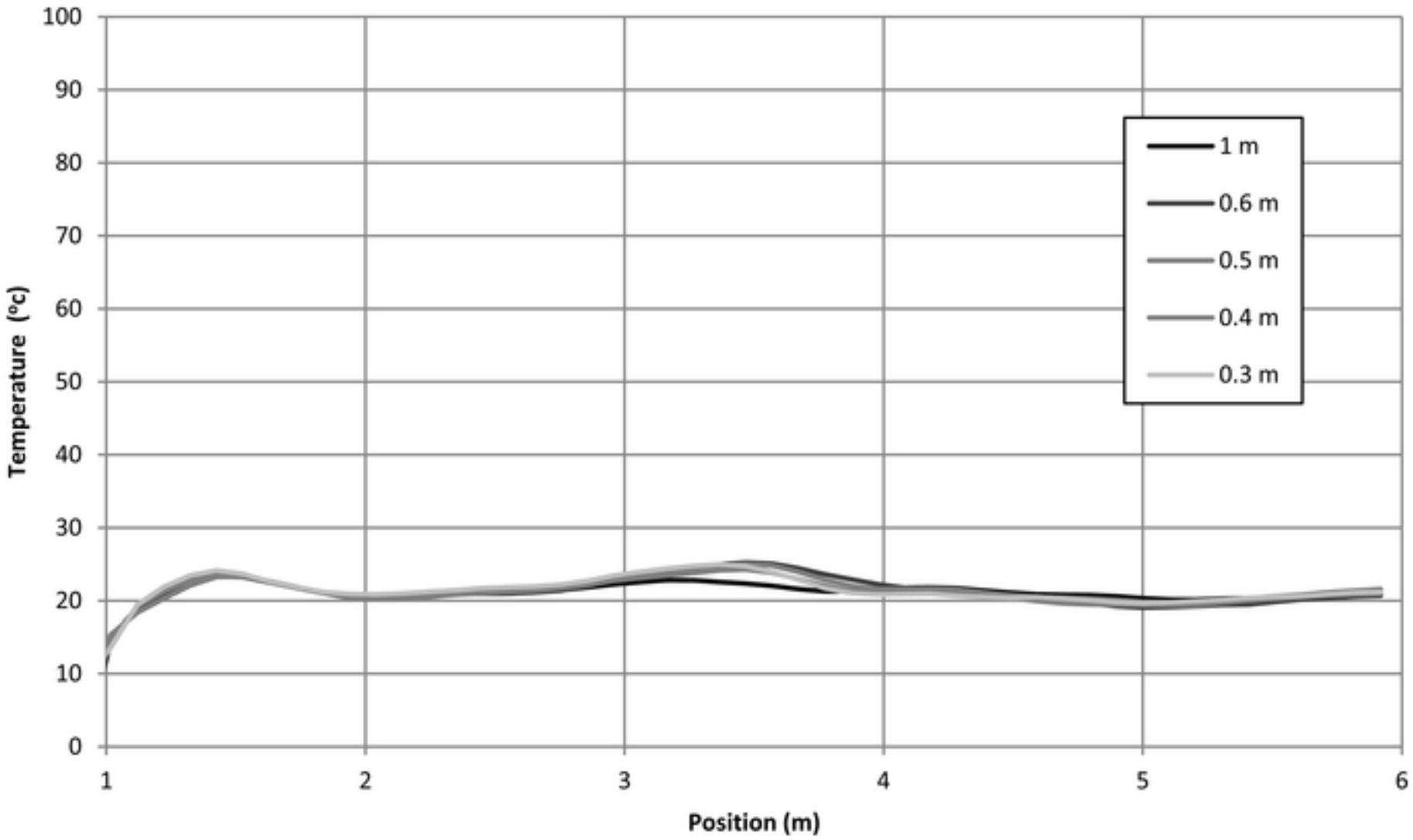

Figure-9
Click here to download high resolution image

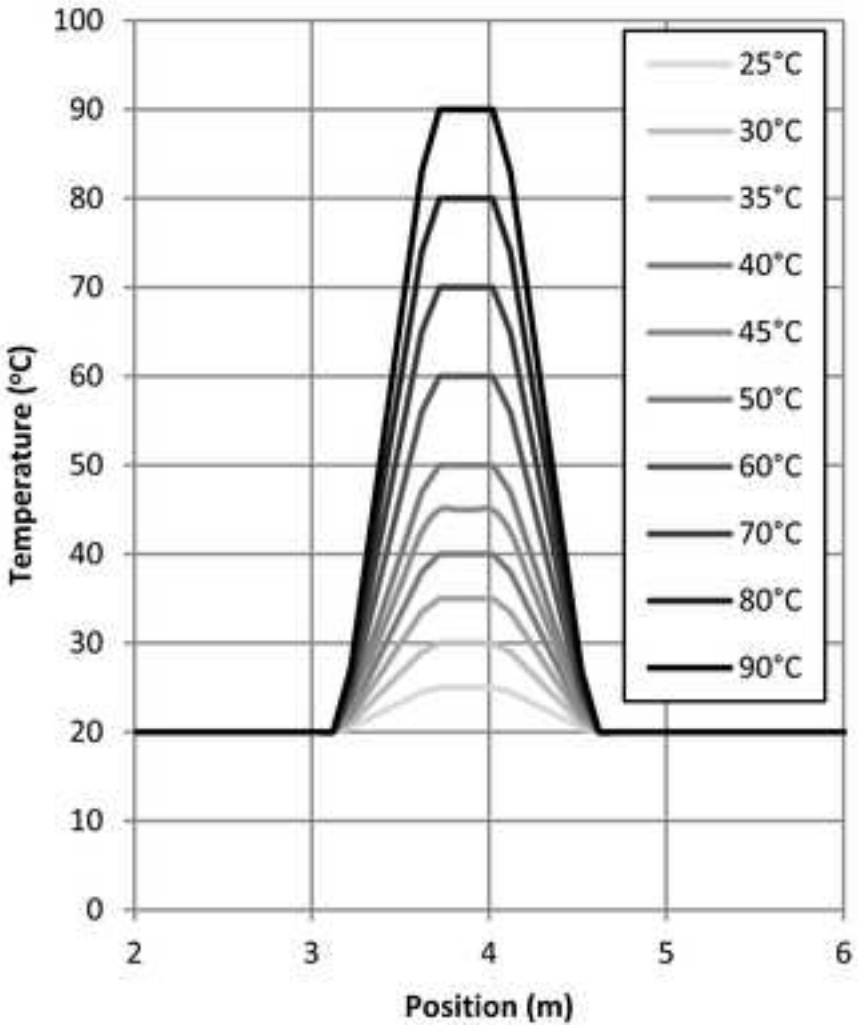

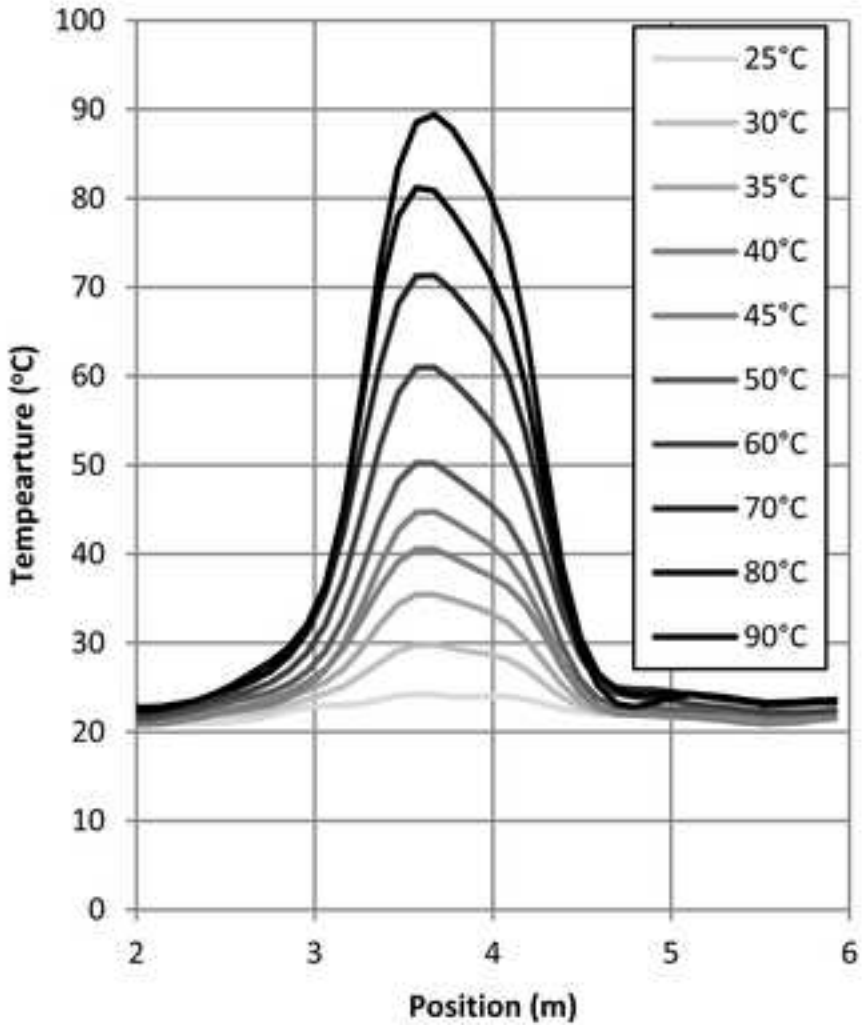

Figure-10
Click here to download high resolution image

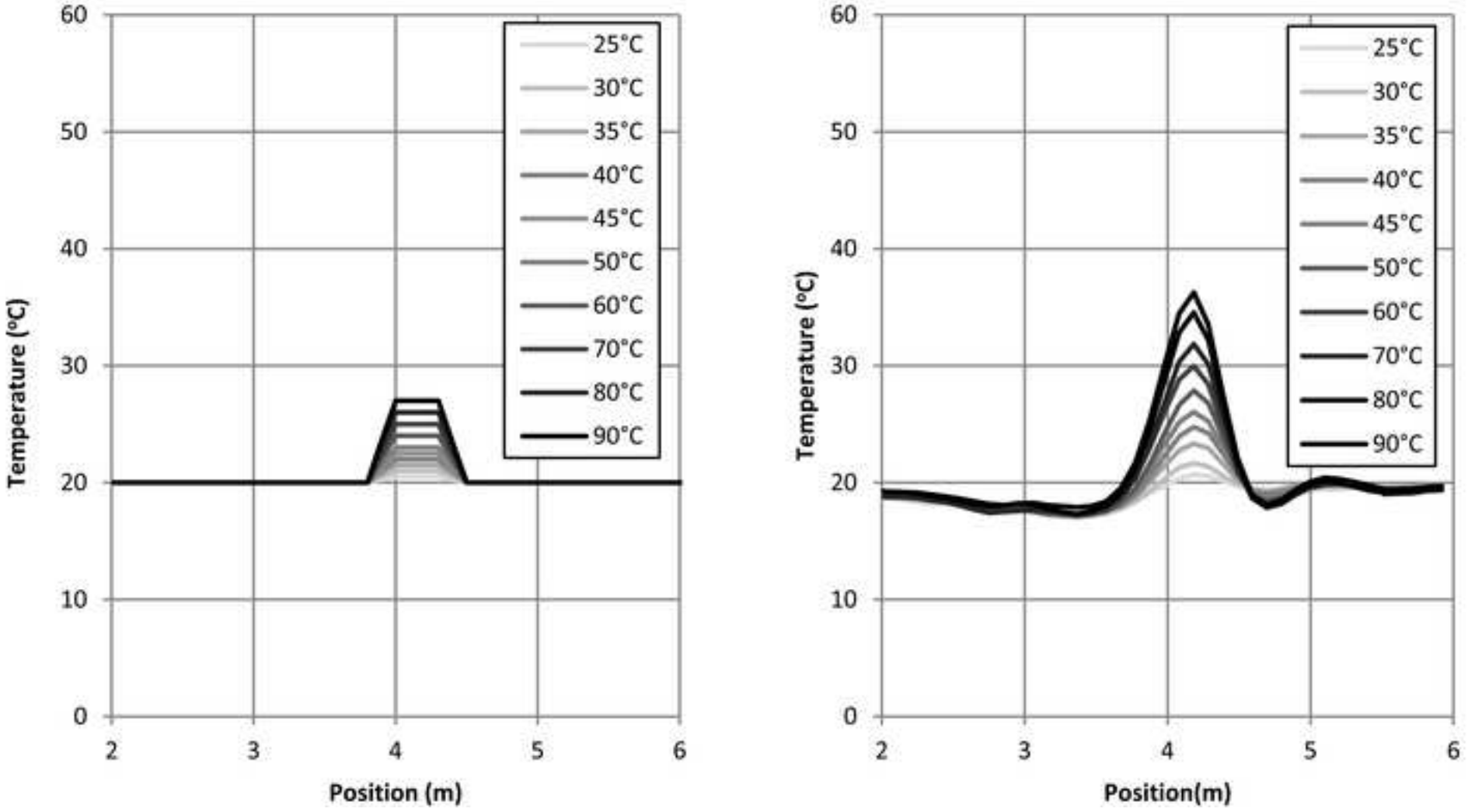

Figure-11
Click here to download high resolution image

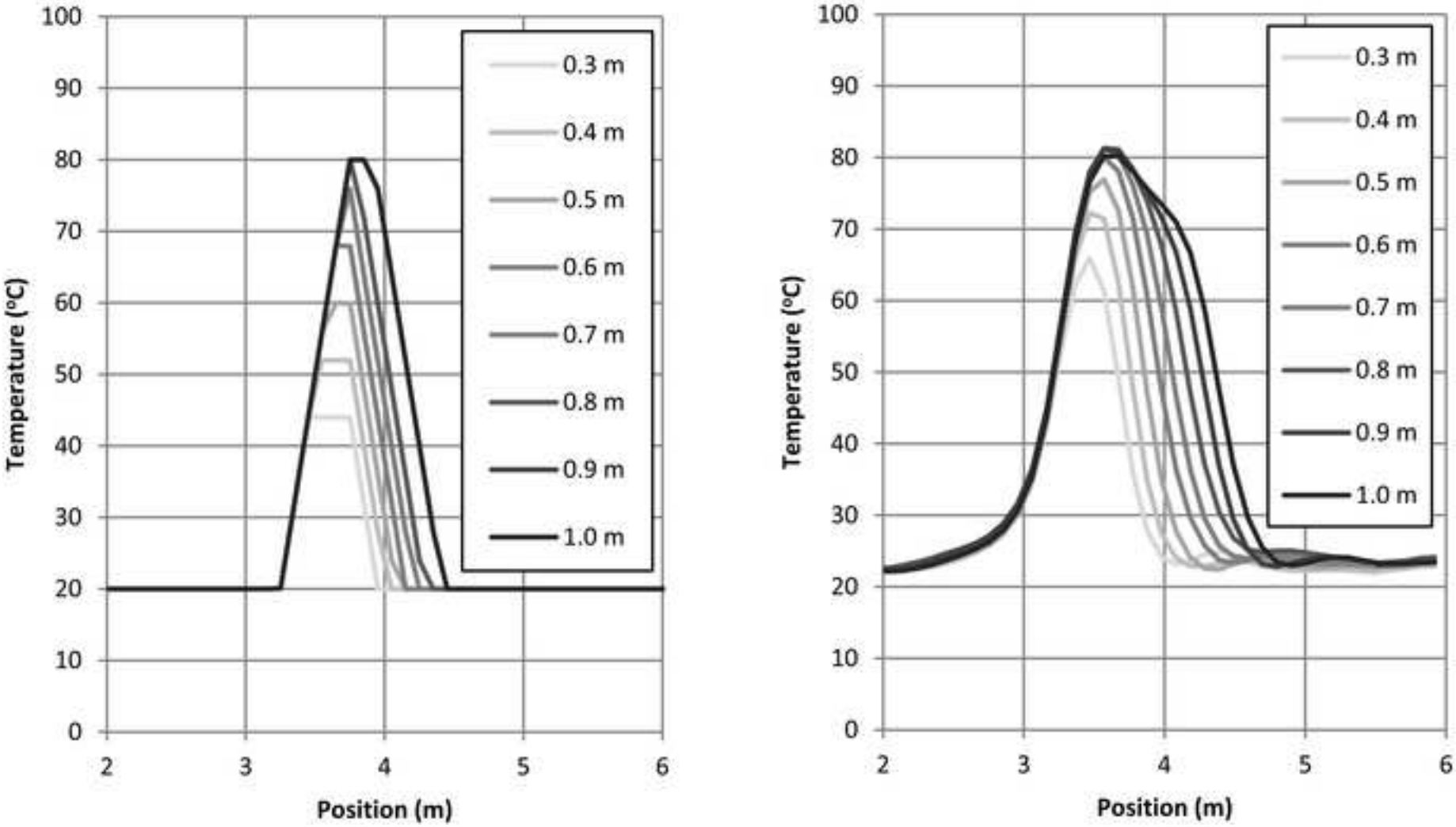

Table 1 Specifications of the fibre-optic cable

Figure 1: Oil Leak from a subsea pipeline (after Goldenberg 2010)

Figure 2: Schematic of different scattering modes in a fibre-optic cable (following Walk and Frings, 2010)

Figure 3: Varying Spatial Resolution – mathematical predictions

Figure 4: Varying increment with spatial resolution – mathematical predictions

Figure 5: Schematic of the experimental setup of the cable a) long heated length b) short heated length

Figure 6: Photographs of the actual experimental setup of the cable a) long heated length b) short heated length

Figure 7: Estimating the time needed for the fibre-optic cable to reach thermal equilibrium-temperature profile with time

Figure 8: Measurement errors induced by mechanical strain

Figure 9: Assessing temperature sensitivity for length longer than spatial resolution a) Theoretical predictions b) Experimental results

Figure 10: Assessing temperature sensitivity for lengths shorter than spatial resolution a) Theoretical predictions b) Experimental results

Figure 11: Assessing spatial sensitivity a) Theoretical predictions b) Experimental results